1. Andriy CHABAN[1,2,3], 2. Marek LIS[4], 3. Andrzej SZAFRANIEC[1], 4. Vitaliy LEVONIUK[3]

Faculty of Transport, Electrical Engineering and Computer Science, University of Technology and Humanities (1), Lviv Politechnik National University (2), Lviv National Agrarian University (3), Faculty of Electrical Engineering, Czestochowa University of Technology (4)
ORCID: 1. 0000-0002-4620-301X; 2. 0000-0001-5191-8303; 3. 0000-0002-0143-2409; 4. 0000-0003-2113-107X

doi:10.15199/48.2022.01.10

The mathematical modelling of transient processes in a drive system including asynchronous and synchronous drives of susceptible motion transmission

Abstract. *A mathematical model is developed of an electric drive system including a power transformer, deep bar cage induction asynchronous motors, and long shaft synchronous drives of distributed mechanical parameters. The model of a deep bar cage induction asynchronous motor addresses the skin-effects across the rotor cage bars using the theory of electromagnetic field. The motion transmission of the drives is described with a mixed problem of the third type Poincaré boundary conditions. The general system of differential equations is given in the Cauchy form, integrated by means of the latent Euler method. Results of computer simulations are shown with graphics, which are analysed.*

Streszczenie. *W pracy niniejszej opracowano model matematyczny zespołu elektrycznego obciążenia, który zawiera transformator mocy, głębokożobkowe napędy asynchroniczne i napędy synchroniczne z długimi wałami o mechanicznych parametrach rozłożonych. Model głębokożłobkowych silników asynchronicznych uwzględnia zjawisko naskórkowości w prętach klatki wirników za pomocą teorii pola elektromagnetycznego. Transmisję ruchu napędów opisuje się za pomocą zadania mieszanego o warunkach brzegowych trzeciego rodzaju Poincaré. Ogólny układ równań różniczkowych podany jest w postaci Cauchy, który całkuje się za pomocą ukrytej metody Eulera. Wyniki symulacji komputerowej przedstawione są w postaci rysunków, które są analizowane. (**Modelowanie matematyczne procesów przejściowych w układzie napędowym obejmującym napędy asynchroniczne i synchroniczne o podatnej transmisji ruchu**)*

Keywords: drive systems, asynchronous drives, synchronous drives, long elastic elements, distributed parameter systems, oscillatory processes, mathematical modelling.
Słowa kluczowe: Układy napędowe, zespól elektrycznego obciążenia, napędy asynchroniczne, napędy synchroniczne, długie elementy sprężyste, układy o parametrach rozłożonych, procesy oscylacyjne, modelowanie matematyczne.

Introduction

The mathematical modelling of drive systems with complicated motion transmissions plays a very important role in the theory of electromechanical dynamic systems. Long driving shafts of distributed mechanical parameters are one such type of the transmissions. The susceptible transmissions of this type are known to exhibit very complicated torsional oscillatory processes, which in some cases leads to the generation of resonant and nearly resonant states in these drives. These processes have adverse effects on the operation not only of single drives but occasionally also on an entire electrical system that includes not only the drives but also other electricity users like lighting, heating, and other [1–4].

It is obvious the oscillatory processes in an electromechanical system need to be addressed at the stages of both design and operation. Experimentation is very costly and, in the case of medium and high-power drives, potentially dangerous to testing personnel. Therefore, some other methods of analysing complicated objects by application of mathematical modelling are rapidly developed at present [2, 5, 6].

The degree of adequacy of mathematical models of dynamic equipment depends on the accuracy of a model, that is, on increasing the number of the degrees of freedom of an object under analysis and on addressing a majority of motions present. For instance, long shafts can be modelled by increasing the number of elementary shaft units or addressing the motion of the mechanical elastic wave along the shaft. The former relies on Lagrange lumped parameter theory, the latter, on Euler-Poisson distributed parameter theory. The latter is evidently more precise [7–9]. It uses a highly complicated mathematical apparatus, on the other hand. We address oscillatory processes in long motion transmission shafts of electric drives here by using the wave equation and considering the third-type boundary conditions.

A mathematical model of a non-linear power transformer is presented that operates symmetrically, its associated fluxes are compensated, i.e., absent from its non-magnetic part. The models of a salient-poled synchronous motor and of a deep bar cage asynchronous motor with a non-linear magnetising curve are discussed as well while addressing current displacement across the rotor cage bars. **The purpose of this paper** is to develop a mathematical model of an electric power system containing a power transformer, deep bar cage asynchronous drives, and salient-poled synchronous drives. All the drives feature complicated motion transmissions, that is, long shafts of distributed mechanical parameters.

The mathematical model of the system.

The electric machine system discussed here is shown in Fig. 1.

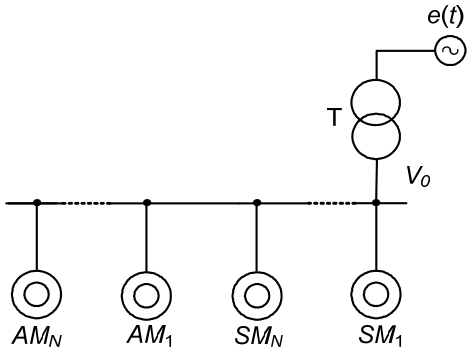

Fig.1. The wiring diagram of the electric machine system

The nomenclature in Fig. 1: $\mathbf{e}(t)$ – the columnar vector of phase electromotive forces of a rigid electric power grid, T – power transformer, $\boldsymbol{V}_0$ – the columnar vector of the drive system's phase voltages, *AM* – asynchronous drives, *SM* – synchronous drives, *N* – the number of asynchronous

drives in the drive system, M – the number of synchronous drives in the drive system.

The motion transmission for both the drive types is depicted in Fig. 2.

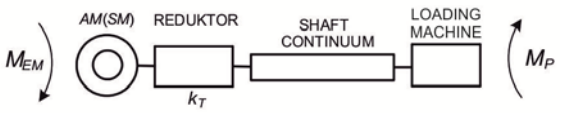

Fig.2. The wiring diagram of the drive system

Fig. 2 includes the following symbols: M_{EM} – the electromagnetic torque of the drive motor, M_P – load moment, k_T – the reducer's gear.

Use of the first Kirchhoff law allows to ignore three-phase equation elements in the model. We assume the electromechanical system in Fig. 1 works in a symmetrical state and uncompensated associated fluxes in the non-magnetic zone of the power transformer can be ignored [2].

A mathematical model of the power transformer

When the power transformer is described with equations, parameters of the primary transformer winding are reduced to those of the secondary winding including the transformer's gear. We'll then write:

(1) $$\frac{d\boldsymbol{\Psi}_1}{dt}=\mathbf{e}(t)-\mathbf{r}_1\mathbf{i}_1\,,\quad \frac{d\boldsymbol{\Psi}_2}{dt}=\mathbf{V}_0-\mathbf{r}_2\mathbf{i}_2\,,$$

where: $\boldsymbol{\Psi}$ – the columnar vectors of full associated fluxes across the transformer, $\mathbf{i}_1,\mathbf{i}_2$ – the columnar vectors of phase currents of the transformer's primary and secondary windings, respectively, $\mathbf{r}$ – the matrices of winding resistances.

Following from the definition of the full associated flux, we note:

(2) $$\mathbf{i}_1=\boldsymbol{\alpha}_{\sigma 1}(\boldsymbol{\Psi}_1-\boldsymbol{\psi}),\quad \mathbf{i}_2=\boldsymbol{\alpha}_{\sigma 2}(\boldsymbol{\Psi}_2-\boldsymbol{\psi})\,,$$

where: $\boldsymbol{\alpha}_{\sigma 1},\boldsymbol{\alpha}_{\sigma 2}$ – the matrices of reverse transformer leakage inductances, $\boldsymbol{\psi}$ – the columnar vector of working associated transformer fluxes.

We'll differentiate (2) in time considering the initial conditions and (1):

(3) $$\frac{d\mathbf{i}_1}{dt}=\boldsymbol{\alpha}_{\sigma 1}\left(\frac{d\boldsymbol{\Psi}_1}{dt}-\frac{d\boldsymbol{\psi}}{dt}\right)=\boldsymbol{\alpha}_{\sigma 1}\left(\mathbf{e}(t)-\mathbf{r}_1\mathbf{i}_1-\frac{d\boldsymbol{\psi}}{dt}\right);$$

(4) $$\frac{d\mathbf{i}_2}{dt}=\boldsymbol{\alpha}_{\sigma 2}\left(\frac{d\boldsymbol{\Psi}_2}{dt}-\frac{d\boldsymbol{\psi}}{dt}\right)=\boldsymbol{\alpha}_{\sigma 2}\left(\mathbf{V}_0-\mathbf{r}_2\mathbf{i}_2-\frac{d\boldsymbol{\psi}}{dt}\right).$$

The columnar vector of working associated fluxes will be presented as defined by [10]:

(5) $$\boldsymbol{\psi}=\boldsymbol{\tau}^{-1}(\mathbf{i}_1+\mathbf{i}_2),\quad \boldsymbol{\tau}=\begin{array}{|c|c|}\hline \tau_A & \\ \hline & \tau_B \\ \hline\end\equiv \operatorname{diag}(\tau_A;\tau_B)\,,$$

where: $\boldsymbol{\tau}$ – the matrix of reverse magnetising inductances of the transformer.

In (5) is then differentiated in time considering the initial conditions:

(6) $$\frac{d\boldsymbol{\psi}}{dt}=\frac{d}{dt}\left(\boldsymbol{\tau}^{-1}(\mathbf{i}_1+\mathbf{i}_2)\right)=\boldsymbol{\tau}^{-1}\frac{d(\mathbf{i}_1+\mathbf{i}_2)}{dt}-$$

$$-\boldsymbol{\tau}^{-2}\frac{d\boldsymbol{\tau}}{dt}(\mathbf{i}_1+\mathbf{i}_2),\quad \boldsymbol{\tau}^{-2}\equiv\boldsymbol{\tau}^{-1}\cdot\boldsymbol{\tau}^{-1},\tau_j=\left(\frac{\psi_j}{i_{1,j}+i_{1,j}}\right)^{-1},\ j=A,B\,.$$

Each component of (3), (4), (6) will be developed as follows:

(7) $$\boldsymbol{\tau}^{-1}\frac{d(\mathbf{i}_1+\mathbf{i}_2)}{dt}=\boldsymbol{\tau}^{-1}\left[\boldsymbol{\alpha}_{\sigma 1}\left(\mathbf{e}(t)-\mathbf{r}_1\mathbf{i}_1-\frac{d\boldsymbol{\psi}}{dt}\right)+\right.$$

$$\left.+\boldsymbol{\alpha}_{\sigma 2}\left(\mathbf{V}_0-\mathbf{r}_2\mathbf{i}_2-\frac{d\boldsymbol{\psi}}{dt}\right)\right];$$

(8) $$\frac{d\boldsymbol{\tau}}{dt}=\frac{\partial\boldsymbol{\tau}}{\partial\boldsymbol{\psi}}\frac{d\boldsymbol{\psi}}{dt}=\frac{\partial}{\partial\boldsymbol{\psi}}\left(\boldsymbol{\psi}^{-1}(\mathbf{i}_1+\mathbf{i}_2)\right)\frac{d\boldsymbol{\psi}}{dt}=\left(\boldsymbol{\psi}^{-1}\frac{\partial(\mathbf{i}_1+\mathbf{i}_2)}{\partial\boldsymbol{\psi}}-\right.$$

$$\left.-\boldsymbol{\psi}^{-2}(\mathbf{i}_1+\mathbf{i}_2)\right)\frac{d\boldsymbol{\psi}}{dt}=\boldsymbol{\psi}^{-1}(\boldsymbol{\rho}-\boldsymbol{\tau})\frac{d\boldsymbol{\psi}}{dt},\qquad \boldsymbol{\rho}\equiv\boldsymbol{\tau}^{\partial}=\frac{\partial(\mathbf{i}_1+\mathbf{i}_2)}{\partial\boldsymbol{\psi}}\,,$$

where: $\boldsymbol{\rho}$ – the matrix of reverse differential magnetising inductances.

(9) $$\boldsymbol{\tau}^{-2}\frac{d\boldsymbol{\tau}}{dt}(\mathbf{i}_1+\mathbf{i}_2)=\boldsymbol{\tau}^{-2}\boldsymbol{\psi}^{-1}(\boldsymbol{\rho}-\boldsymbol{\tau})(\mathbf{i}_1+\mathbf{i}_2)\frac{d\boldsymbol{\psi}}{dt}=\boldsymbol{\tau}^{-1}(\boldsymbol{\rho}-\boldsymbol{\tau})\frac{d\boldsymbol{\psi}}{dt}\,.$$

(9) will result in:

(10) $$\frac{d\boldsymbol{\psi}}{dt}=\mathbf{G}_1\left(\mathbf{e}(t)-\mathbf{r}_1\mathbf{i}_1\right)+\mathbf{G}_2\left(\mathbf{V}_0-\mathbf{r}_2\mathbf{i}_2\right),$$

where:

(11) $$\mathbf{G}\equiv\begin{array}{|c|c|}\hline (\alpha_{\sigma 1A}+\alpha_{\sigma 2A}+\rho_A)^{-1} & \\ \hline & (\alpha_{\sigma 1B}+\alpha_{\sigma 2B}+\rho_B)^{-1} \\ \hline\end;$$

(12) $$\mathbf{G}_1=\boldsymbol{\alpha}_{\sigma 1}\mathbf{G},\ \mathbf{G}_2=\boldsymbol{\alpha}_{\sigma 2}\mathbf{G},\ \rho_i=\left(\frac{\partial\psi_j}{\partial(i_{1,j}+i_{2,j})}\right)^{-1},\ j=A,B\,.$$

The derivative of the columnar vector of the secondary winding current is determined from the equation, cf. (3):

(13) $$\frac{d\mathbf{i}_2}{dt}=\boldsymbol{\alpha}_{\sigma 2}\left((\mathbf{1}-\mathbf{G}_2)\mathbf{V}_0-\mathbf{G}_1\left(\mathbf{e}(t)-\mathbf{r}_1\mathbf{i}_1\right)-(\mathbf{1}-\mathbf{G}_2)\mathbf{r}_2\mathbf{i}_2\right).$$

A mathematical model of the asynchronous motors

The concept of the model of an asynchronous motor is similar to that of the power transformer. The parameters of the rotor winding are reduced to those of the stator winding considering the current and voltage gears k_i, k_u. Deep bar cage asynchronous motors are adopted for the purposes of analysis, where the current displacement across the rotor bars is addressed [9,10] on the basis of the theory of electromagnetic field, which allows to calculate the voltage across the rotor bars using ordinary and partial derivative equations [10].

The equations of asynchronous motor [10]:

(14) $$\frac{d\boldsymbol{\Psi}_{S,n}}{dt}=\mathbf{V}_0-\mathbf{r}_{S,n}\boldsymbol{\alpha}_{\sigma S,n}(\boldsymbol{\Psi}_{S,n}-\boldsymbol{\psi}_n)\,;$$

(15) $$\frac{d\boldsymbol{\Psi}_{R,n}}{dt}=-\mathbf{u}_{R,n}-\mathbf{r}_{RL,n}\boldsymbol{\alpha}_{\sigma RL,n}(\boldsymbol{\Psi}_{R,n}-\boldsymbol{\Pi}_n^{-1}\boldsymbol{\psi}_n)\,;$$

(16) $$\frac{d\boldsymbol{\psi}_n}{dt}=\mathbf{G}_{S,n}\left(\mathbf{V}_0-\mathbf{r}_{S,n}i_{S,n}\right)+$$

$$+\mathbf{G}_{R,n}\left(-\mathbf{u}_{R,n}-\mathbf{r}_{RL,n}\mathbf{i}_{R,n}-\boldsymbol{\Omega}_n\boldsymbol{\Psi}_{R,n}\right),$$

where: $\mathbf{G}_{S,n}$, $\mathbf{G}_{R,n}$ – transformation matrices.

The currents across the motor will be determined in the ordinary manner, see (2):

(17) $$\mathbf{i}_{S,n}=\boldsymbol{\alpha}_{\sigma S,n}(\boldsymbol{\Psi}_{S,n}-\boldsymbol{\psi}_n),\quad \mathbf{i}_{R,n}=\boldsymbol{\alpha}_{\sigma RL,n}(\boldsymbol{\Psi}_{R,n}-\boldsymbol{\Pi}_n^{-1}\boldsymbol{\psi}_n)\,.$$

where: $\boldsymbol{\Pi}$ – the matrix of oblique transformations, $\boldsymbol{\Omega}$ – the matrix of the angular rotational speeds of the asynchronous motor in oblique coordinates, S and R – the indices for the stator and rotor, $\mathbf{u}_R$ – the columnar vector of voltages across the rotor cage bars, $k=N$ – the number of asynchronous motors in the drive system.

Differentiating the first expression of (17) in time and considering (14) and (16) will produce:

(18) $$\frac{d\mathbf{i}_{S,n}}{dt}=\mathbf{A}_{S,n}(\mathbf{V}_0-\mathbf{r}_{S,n}\mathbf{i}_{S,n})+\mathbf{A}_{SR,n}(-\mathbf{u}_{R,n}-$$
$$-\boldsymbol{\Omega}_n\boldsymbol{\Psi}_{R,n}-\mathbf{r}_{RL,n}\mathbf{i}_{R,n}),$$

where: $\mathbf{A}_S$, $\mathbf{A}_{SR}$ – the matrices of reverse inductances.

Voltages across the rotor cage bars will be determined according to Maxwell's theory and the theorem of voltage on the bar wire surface [10].

(19) $$\frac{\partial\mathbf{H}}{\partial t}=-\frac{\nu}{\gamma}\nabla\times\nabla\times\mathbf{H},\ \mathbf{E}=\frac{1}{\gamma}\nabla\times\mathbf{H},\ \mathbf{u}_R=\mathbf{E}(0)l,\ \nu=\frac{1}{\mu},$$

where: $\mathbf{E}(0)$ – electric field intensity on the bar surface, l – the length of a bar.

Boundary conditions for the first equation in (19) will be expressed according to the law of current surge [3, 10]:

(20) $$H_j\Big|_{z=0}=\frac{i_{R,n}}{a},\quad H_j\Big|_{z=h}=0,\quad j=A,B.$$

The discretisation of the first expression in (19) by means of the straight-line method will produce [3, 10]:

(21) $$\frac{dH_{j,n}}{dt}=\frac{\nu}{\gamma(\Delta z)^2}(H_{j,n-1}-2H_{j,n}+H_{j,n+1})\ \ j=A,B,$$

where: $n=2,3,...,T-1$, $\Delta z=h/(T-1)$ – discretisation step, T – the number of discretisation nodes relative to the coordinate z. Normally, $T\geq10$, a – bar width, h – bar depth relative to the coordinate z.

The voltage across the rotor cage bars, see (19), is:

(22) $$u_{R,j}=-l\frac{k_uk_i}{2\gamma\Delta z}(-3H_{j,1}+4H_{j,2}-H_{j,3}),\qquad j=A,B.$$

The electromagnetic torque of the asynchronous motor will be determined from [9]:

(23) $$M_{EM}=\sqrt{3}p_0\alpha_{\sigma S}(\Psi_{SB}\Psi^{\Pi}_{RA}-\Psi_{SA}\Psi^{\Pi}_{RB}),$$

where: p_0– the number of machine pole pairs.

A mathematical model of the synchronous motors

The parameters of the stator winding are reduced to those of the rotor winding considering the current and voltage gears k_i, k_u. Synchronous motors including salient-pole rotors are analysed. Three currents flow across the rotor of the modelled motor: two (excitation and damping currents along the d-d axis) across the longitudinal d-d axis and one along the transverse q-q axis (damping current along the q-q axis), while the C phase current is excluded from the stator. In the event, a topological matrix **B** is introduced in order to fulfil the law of matrix multiplication.

(24) $$\frac{d\boldsymbol{\Psi}_{S,m}}{dt}=\mathbf{V}_0-\mathbf{r}_{S,m}\boldsymbol{\alpha}_{\sigma S,m}(\boldsymbol{\Psi}_{S,m}-\boldsymbol{\Pi}^{-1}_{1,m}\boldsymbol{\psi}_m);$$

(25) $$\frac{d\boldsymbol{\Psi}_{R,m}}{dt}=\mathbf{u}_{R,m}-\mathbf{r}_{R,m}\boldsymbol{\alpha}_{\sigma R,m}(\boldsymbol{\Psi}_{R,m}-\mathbf{B}_m\boldsymbol{\psi}_m);$$

(26) $$\mathbf{i}_{S,m}=\boldsymbol{\alpha}_{\sigma S,m}(\boldsymbol{\Psi}_{S,m}-\boldsymbol{\Pi}^{-1}_{1,m}\boldsymbol{\psi}_m);$$

(27) $$\mathbf{i}_{R,m}=\boldsymbol{\alpha}_{\sigma R,m}(\boldsymbol{\Psi}_{R,m}-\mathbf{B}_m\boldsymbol{\psi}_m);$$

(28) $$\frac{d\boldsymbol{\psi}_m}{dt}=\mathbf{G}_{S,m}\left(\mathbf{V}_0-\boldsymbol{\Omega}_m\boldsymbol{\Psi}_{S,m}-\mathbf{r}_{S,m}i_{S,m}\right)+$$
$$+\mathbf{G}_{R,n}\mathbf{B}^{\mathrm{T}}(\mathbf{u}_{R,m}-\mathbf{r}_{R,m}\mathbf{i}_{R,m}).$$

Differentiating the first expression in (26) over time and considering (24) and (28) produces:

(29) $$\frac{d\mathbf{i}_{S,m}}{dt}=\mathbf{A}_{S,m}(\mathbf{V}_0-\mathbf{r}_{S,m}\mathbf{i}_{S,m}-\boldsymbol{\Omega}_m\boldsymbol{\Psi}_{S,m})+$$
$$+\mathbf{A}_{SR,m}\mathbf{B}^{\mathrm{T}}(\mathbf{u}_{R,m}-\mathbf{r}_{R,m}\mathbf{i}_{R,m})+\boldsymbol{\Omega}_m\mathbf{i}_{S,m},\ \mathbf{B}^{\mathrm{T}}\equiv\begin{bmatrix}1&&1\\&1&\end{bmatrix},$$

where: $\boldsymbol{\Omega}_1$ – the matrix of the angular rotational speeds of the synchronous machine in two-dimensional coordinates, $\boldsymbol{\Pi}_1$ – Park matrix of two-dimensional transformations, $m = M$ – the number of synchronous motors in the drive system.

The electromagnetic torque of the synchronous motor will be determined from [10]:

(30) $$M_{EM}=\sqrt{3}k_Tp_0(\psi_{SB}i_{SA}-\psi_{SA}i_{SB}).$$

Motion transmissions in asynchronous and synchronous drives are presented as elastic elements of distributed parameters. A calculation scheme of motion transmission will be introduced for the purpose of modelling the mechanical subsystem in Fig. 3.

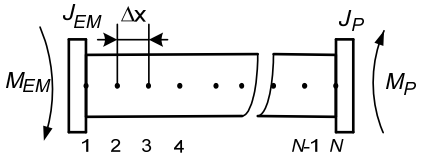

Fig.3. A calculation scheme of the long shaft

The designations in Fig. 3: M_{EM} – electromagnetic torque of the drive motor, M_P – pump's hydraulic torque, J_{EM} – the drive rotor's moment of inertia, J_P – the drive machine rotor's moment of inertia converted considering the reducer gear, Δx – the discretisation step of the long shaft equation, N – the number of discretisation nodes.

This is the equation of long shaft oscillations in the motion transmission and the boundary conditions for this equation [4,11].

(31) $$\frac{\partial^2\varphi(x,t)}{\partial t^2}=\frac{G}{\rho}\frac{\partial^2\varphi(x,t)}{\partial x^2}+\frac{\xi}{\rho J_p}\frac{\partial^2\varphi(x,t)}{\partial x^2},$$

where: G – shear modulus, ξ – the coefficient of shaft internal leakage, x – current coordinate along the shaft, ρ – the density of the shaft material, J_p – the shaft's polar moment of inertia, $\varphi(x,t)$ – the angle of shaft rotation.

Poincaré boundary conditions of the third type [4], formulated on the basis of d'Alembert law [10], cf. Fig. 2, 3, will be attached to the shaft equation:

(32) $$k_T^{-2}J_{EM}\frac{d\omega_1}{dt}-GJ_p\frac{\partial\varphi}{\partial x}\Big|_{x=0}-\xi\frac{\partial^2\varphi}{\partial x\partial t}\Big|_{x=0}=k_T^{-1}M_{EM};$$

(33) $$GJ_p\frac{\partial\varphi}{\partial x}\Big|_{x=L}+\xi\frac{\partial^2\varphi}{\partial x\partial t}\Big|_{x=L}-J_P\frac{d\omega_{90}}{dt}=M_P,\quad k_T=\frac{\omega_1}{\omega_R},$$

where: φ_R – the angle of the rotor rotation, ω_R – the angular velocity of the rotor.

Discretisation of (31) – (33) with the straight-line method will produce:

(34) $$\frac{d\omega_1}{dt}=\frac{2\left(k_T^{-1}M_{EM}\Delta x-J_pG(\varphi_1-\varphi_2)-\xi(\omega_1-\omega_2)\right)}{\left(J_p\rho\Delta x+2k_T^{-2}J_{EM}\right)\Delta x};$$

(35) $$\frac{d\omega_i}{dt}=\frac{G}{\rho}\frac{\varphi_{i-1}-2\varphi_i+\varphi_{i+1}}{(\Delta x)^2}+$$
$$+\frac{\xi}{\rho J_p}\frac{\omega_{i-1}-2\omega_i+\omega_{i+1}}{(\Delta x)^2},\quad i=2,3...,89;$$

(36) $$\frac{d\omega_N}{dt}=\frac{2\left(M_P\Delta x+J_pG(\varphi_{N-1}-\varphi_N)+\xi(\omega_{N-1}-\omega_N)\right)}{\left(J_p\rho\Delta x+2J_P\right)\Delta x};$$

(37) $$\frac{d\varphi_i}{dt}=\omega_i,\quad i=1,2,...,N.$$

An unknown function $\mathbf{V}_0$ – the voltage of the loading system, is present in (1), (14), (24). To find the voltage, the first Kirchhoff law will be differentiated in time considering the initial conditions, see Fig. 1:

$$\frac{d\mathbf{i}_2}{dt}+\frac{d}{dt}\sum_{n=1}^{N}\mathbf{i}_{S,n}+\frac{d}{dt}\sum_{m=1}^{M}\mathbf{i}_{S,m}=0\,. \tag{38}$$

By substituting (13), (18), (29) to (38), the function of the system voltage results:

$$\mathbf{V}=\left\{\boldsymbol{\alpha}_{\sigma 2}(\mathbf{1}-\mathbf{G}_2)+\sum_{n=1}^{N}\mathbf{A}_{S,n}+\sum_{m=1}^{M}\mathbf{A}_{S,m}\right\}^{-1}\left\{\boldsymbol{\alpha}_{\sigma 2}\left((\mathbf{G}_2-\mathbf{1})\times\right.\right. \tag{39}$$

$$\times\mathbf{r}_2\mathbf{i}_2+\mathbf{G}_1\left(\mathbf{e}(t)-\mathbf{r}_1\mathbf{i}_1\right)\Big)+\sum_{n=1}^{N}\Big[\mathbf{A}_{S,n}\mathbf{r}_{S,n}\mathbf{i}_{S,n}-\mathbf{A}_{SR,n}(-\mathbf{u}_{R,n}-$$

$$-\boldsymbol{\Omega}_{1,n}\boldsymbol{\Psi}_{R,n}-\mathbf{r}_{R,n}\mathbf{i}_{R,n})\Big]+\sum_{m=1}^{M}\Big[\mathbf{A}_{S,m}(\mathbf{r}_{S,m}\mathbf{i}_{S,m}-\boldsymbol{\Omega}_m\boldsymbol{\Psi}_{S,m})-$$

$$\left.\left.-\mathbf{A}_{SR,m}(\mathbf{u}_{R,m}-\mathbf{r}_{R,m}\mathbf{i}_{R,m})-\boldsymbol{\Omega}_m\mathbf{i}_{S,m}\Big]\right\}\right..$$

The following equations: (1), (10), (14) – (16), (21), (24), (25), (28), (34) – (37) are jointly integrated considering: (2), (11), (12), (17), (22), (23), (26), (27), (30), (39).

The results of computer simulation

The computer simulation is undertaken for the electric system whose diagram is shown in Fig. 1 – 3. The operation of two deep bar cage induction asynchronous motors and a single synchronous motor is taken into account. These are the parameters of the system: power transformer type TM-1600 (1.6 MVA; 35/6.3 kV); synchronous motor: SDZB 13-52-8, P_N=630kW, n_N = 750 rpm; U_N = 6 kV; u_f = 42 V, p_0 = 4, J_1 = 1700 kg·m^2, which drives a vertical pump type OB 2-87 with a load moment $M_P = 3{,}958\cdot\omega_2^{1{,}856}$ via a reducer with a gear k_T = 585/750. The shaft dimensions: length L=4.5 m, diameter D=0.12 m. The drive system includes two identical deep bar cage induction asynchronous motors of the type 12-52-8A, P_N = 320 kW, U_N = 6 kV, I_N = 39 A which use the reducers and the long shafts to drive: the first motor drives a vertical pump type OB 16-87 with a load moment M_{P1}=18.449ω+0.691ω^2, while the other motor drives a machine with a constant moment M_{P2}=5000 N·m. The dimensions of the first shaft: L=4.5m, D=0.09m and of the second: L=4.5m, D=0.10m. The gear of both the reducers is k_T = 585/750.

The analysis of electromechanical transient processes proceeds as follows. The synchronous motor is supplied by the secondary winding of the power transformer, whereas the asynchronous drives are connected to the drive system once the synchronous motor enters its synchronous state. The synchronous motor is started when the pump pipeline valve is shut. The excitation winding is short-circuited by a low resistance. Once a sub-synchronous speed is reached, the rotor's excitation winding is switched to a DC source and the pump valve is opened at t=30s. After the motor is in the synchronous state, two asynchronous drives are switched on simultaneously at t=40s.

All the mechanical parameters of the three drives are converted by reducer gears to the input vertical pump shaft considering the gear. The system of ordinary differential equations is integrated by means of the latent Euler method.

Fig. 4 shows the waveforms of the angular velocity of the synchronous motor SM and of the asynchronous motors AM as a function of time during the start-up.

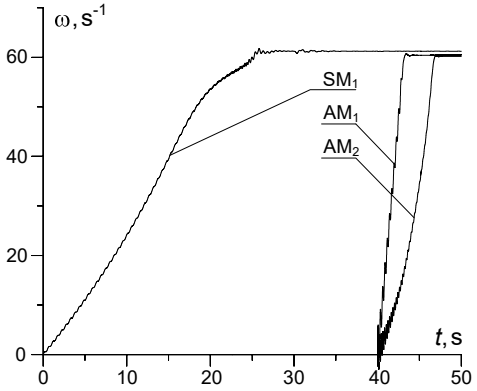

Fig. 4. The start-up of all the electric drives as a function of time

At t=30s, the motor's excitation winding is supplied with the rated voltage, which causes the motor to switch from its sub-synchronous to the synchronous state, The asynchronous drives are then turned on at t=40 s.

Fig. 5 illustrates the waveforms of the angular velocity of the asynchronous motors AM as a function of time.

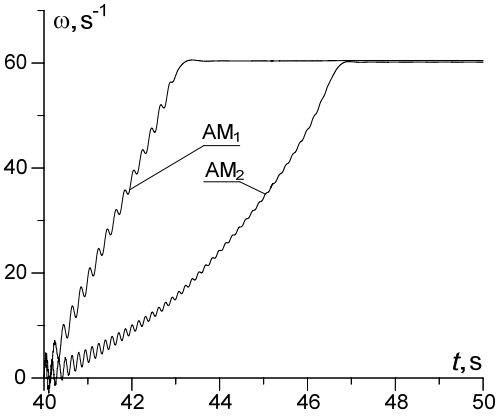

Fig. 5. The start-up of the asynchronous drives as a function of time

Since AM_2 is loaded with a greater moment than AM_1, the time it takes the former to enter its steady state is about twice longer. The different oscillations of rotor speeds of the input shafts of both the asynchronous drives can be noted as well, dependent on the thicknesses of the two long shafts.

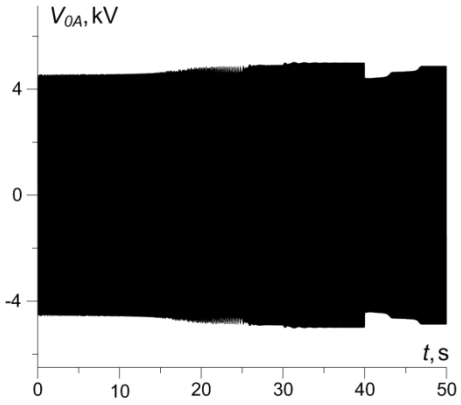

Fig. 6. The instantaneous phase A voltage of the electromechanical system

Fig. 6 and 7 depict the instantaneous phase A voltage of the electromechanical system and the phase A current of the power transformer secondary winding.

During the asynchronous start-up of the synchronous drives, the voltage is below rated because the start-up current is several times larger than the rated current – cf.

Fig. 7. After the motor enters its synchronous state, two asynchronous drives are switched on at t=40 s. Where the three motors are in operation, the high start-up currents of the asynchronous motors cause a reduction of the voltage supplied to the motors.

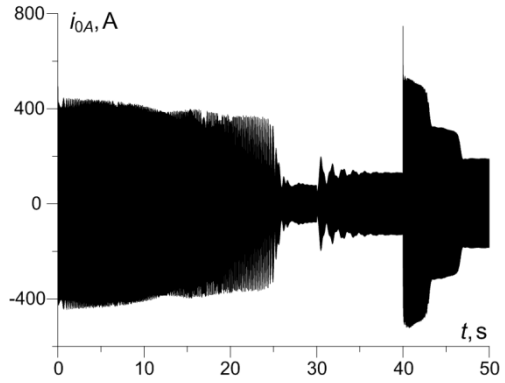

Fig. 7. Phase A current of the power transformer secondary winding

Fig. 8 shows an instantaneous moment of torsion in the middle section of the long motion transmission shaft of the synchronous drive. The oscillatory processes of the moment, whose frequency depends on the shaft thickness, can be noted at the motor's start-up. The moment becomes constant in the steady state for t > 50 s, on the other hand.

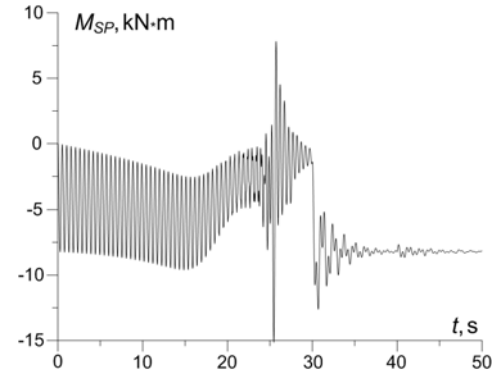

Fig. 8. Instantaneous moment of torsion in the middle section of the synchronous drive motion transmission long shaft.

It should be also pointed out the general operating condition of the electromechanical system is to a great extent affected by resonant and near-resonant processes (rumbling vibrations) described in [3,10,11,13].

Conclusion

The application of the theory of mathematical modelling of dynamic electromagnetic processes in drive systems helps to adequately present physical processes in complicated electric systems including drives with susceptible motion transmission.

The application of the modelling theory to distributed parameter systems in order to describe the impact of skin effects across asynchronous rotor bars allows for addressing the increases of start-up moment.

We analyse drive systems including complicated motion transmissions containing long elastic elements as systems of distributed mechanical parameters, which enables to address the motion of mechanical wave along the shaft.

In electric systems where electromechanical energy conversion is present, the method of modelling proposed here allows for considering virtually all latent motions, since each system element influences the other elements.

The use of synchronous drives in high and medium-power drive systems is advisable as it helps stabilise voltage in the systems of electromechanical energy conversion. In steady processes, this stabilisation applies to the compensation of passive power.

Authors: *dr hab. inż. Andriy Chaban, prof. UTH Rad., Uniwersytet Technologiczno – Humanistyczny, Wydział Transportu, Elektrotechniki i Informatyki, ul. Malczewskiego 29, 26-600 Radom, Politechnika Lwowska, ul Bandery 12, Lwów, Ukraina, E-mail: atchaban@gmail.com;dr hab. inż. Marek Lis prof. PCz., Politechnika Częstochowska, Wydział Elektryczny, 42-201 Czestochowa, al. Armii Krajowej 17, e-mail: marek.lis@pcz.pl; dr inż. Andrzej Szafraniec, prof. UTH Rad., Uniwersytet Technologiczno – Humanistyczny, Wydział Transportu, Elektrotechniki i Informatyki, ul. Malczewskiego 29, 26-600 Radom, E-mail: a.szafraniec@uthrad.pl; dr inż. Vitaliy Levoniuk, Lwowski Narodowy Uniwersytet Rolniczy, ul. W. Wielkiego 1, Dubliany, E-mail: Bacha1991@uk.*

REFERENCES

[1] Ekemb G., Slaoui-Hasnaoui F., Song-Manguelle J., Lingom P., Fofana I., Instantaneous Electromagnetic Torque Components in Synchronous Motors Fed by Load-Commutated Inverters, *Energies,* (2021), No. 14, 3223

[2] Popenda A., Lis M., Nowak M., Blecharz K., Mathematical Modelling of Drive System with an Elastic Coupling Based on Formal Analogy between the Transmission Shaft and the Electric Transmission Line. *Energies, (*2020), No. 13, 1181

[3] Chaban A., Lis M., Szafraniec A., Jedynak R., Application of Genetic Algorithm Elements to Modelling of Rotation Processes in Motion Transmission Including a Long Shaft. *Energies* (2020), No. 14, 115

[4] Pukach P.Y., Kuzio I.V., Nytrebych Z.M., Ilkiv V.S. Analytical methods for determining the effect of the dynamic process on the nonlinear flexural vibrations and the strength of compressed shaft. *Naukovyi Visnyk Natsionalnoho Hirnychoho Universytetu,* (2017), No. 5, 69–76

[5] Czaban A., Rusek, A,, Lis M. The approach based on variation principles for mathematical modeling of asymmetrical states in a power transformer, *Przegląd Elektrotechniczny*, 88 (2012), nr 12B, 240–242

[6] Lis, M.; Chaban, A.; Szafraniec, A.; Figura, R.; Levoniuk, V. Mathematical model of a part of an opened extra-high voltage electrical grid. *E3S Web of Conferences* 2019, *Volume 84*, 02005.

[7] Ziemiński R., Analiza drgań swobodnych pełnego układu dyskretno-ciągłego, Zeszyty Naukowe *A.G.H.*, (1980), nr 775, 177–188

[8] Chaban A., Szafraniec A., Levoniuk V., Mathematical modelling of transient processes in power systems considering effect of high-voltage circuit breakers, *Przegląd Elektrotechniczny*, 95 (2019), nr 1, 49–52

[9] Łukasik Z., Czaban A., Szafraniec, A., Żuk W., The mathematical model of the drive system with asynchronous motor and vertical pump, *Przegląd Elektrotechniczny*, 94 (2018), nr 1, 133–138

[10] Chaban A., Hamilton - Ostrogradski Principle in Electromechanical Systems; *Soroki*, Lviv, Ukraine, (2015), 488

[11] Lozynskyy A., Chaban A., Perzyński T., Szafraniec A., Kasha L., Application of Fractional-Order Calculus to Improve the Mathematical Model of a Two-Mass System with a Long Shaft, *Energies*, (2021), No. 14, 1854

[12] Ortega R., Loria A., Nicklasson P.J., Sira-Ramirez H., Passivity-Beast Control of Euler-Lagrange Systems: Mechanical, Electrical and Electromechanical Applications, London, *Springer Verlag*, (1998), 543

[13] Chaban A., Łukasik, Z., Popenda A., Szafraniec A., Mathematical Modelling of Transient Processes in an Asynchronous Drive with a Long Shaft Including Cardan Joints, *Energies,* (2021), No. 14, 5692